Accepted Manuscript

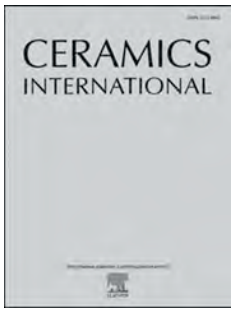

Structure, phase composition, Raman spectra, and microwave dielectric properties of novel $Co_{0.5}Zr_{0.5}TaO_4$ ceramics

Hongyu Yang, Shuren Zhang, Hongcheng Yang, Ying Yuan, Enzhu Li

PII: S0272-8842(19)31142-3

DOI: https://doi.org/10.1016/j.ceramint.2019.05.044

Reference: CERI 21496

To appear in: *Ceramics International*

Received Date: 10 March 2019

Revised Date: 30 April 2019

Accepted Date: 6 May 2019

Please cite this article as: H. Yang, S. Zhang, H. Yang, Y. Yuan, E. Li, Structure, phase composition, Raman spectra, and microwave dielectric properties of novel $Co_{0.5}Zr_{0.5}TaO_4$ ceramics, *Ceramics International* (2019), doi: https://doi.org/10.1016/j.ceramint.2019.05.044.

Structure, Phase composition, Raman spectra, and microwave dielectric properties of novel $Co_{0.5}Zr_{0.5}TaO_4$ ceramics

Hongyu Yang[1,2], Shuren Zhang[*,1,2], Hongcheng Yang[1,2], Ying Yuan[1,2], Enzhu Li[*,1,2]

1. National Engineering Research Center of Electromagnetic Radiation Control Materials, University of Electronic Science and Technology of China, Chengdu
2. Key Laboratory of Multi-Spectral Absorbing Materials and Structures of Ministry of Education, University of Electronic Science and Technology of China, Chengdu, 610054

Corresponding authors: Email: zsr@uestc.edu.cn (Shuren Zhang)
lienzhu@uestc.edu.cn (Enzhu Li)

Abstract

In this study, the crystal structure, phase composition, Raman spectrum, and microwave dielectric properties of novel $Co_{0.5}Zr_{0.5}TaO_4$ ceramics were investigated. Based on the X-ray diffraction, Rietveld refinement analysis and Raman spectroscopy, a coexistence of monoclinic-type and trirutile tetragonal phases was confirmed in the temperature range of 1100~1200 ^oC. The variations of relative density, growth of grain, and contents of each phase are mainly responsible for the developments of microwave dielectric properties of $Co_{0.5}Zr_{0.5}TaO_4$ ceramics. Excellent microwave dielectric properties with a ε_r of 20.19, a Q×f about 65125 GHz and a τ_f ca. of -39.02 ppm/^oC were obtained when sintered at 1150^oC.

Key words: microwave dielectric ceramic; sintering; dielectric properties

1. Introduction

Increasing developments of electronic communication industry promote huge demands of electronic devices[1]. Microwave dielectric materials, especially niobate-based ceramics, such as Li_2O-MO-Nb_2O_5 (M=Zn, Mg)[2-4], MO-M'O_2-Nb_2O_5 (M=Zn, Mg, Co, M'=Ti, Zr)[5-7] have becoming research spots due to their tunable dielectric properties, including an appropriate ε_r and a great Q×f value.

Nowadays, many novel tantalum-based systems with excellent microwave dielectric properties are emerging as worldwide research concerns. For instance, ixiolite-type $ZnTiTa_2O_8$ ceramics with a ε_r of ~ 35.7, a Q×f of 57550 GHz, and a τ_f of ~ -24.7 ppm/^oC were synthesized using sol-gel technology[8]. $ZnZrTa_2O_8$ ceramic with wolframite structure was reported with a Q×f value about 110700 GHz and a ε_r of ~32[9]. Xia reported that wolframite $MgZrTa_2O_8$ ceramics with a ε_r of ~22.76, a Q×f of 131500 GHz and a τ_f ca. of -33.81 ppm/^oC were obtained when sintered at 1475^oC. However, the Q×f value was deteriorated to 39000 GHz when 0.5 wt. % CaF_2 sintering aid was added[10, 11].

In our previous study, novel trirutile-type $Co_{0.5}Ti_{0.5}TaO_4$ solid solution was synthesized, whose microwave dielectric performances are susceptible to sinterability, ionic occupying environment and chemical bond types of crystal structure based on

structural characterizations. Specially, it presents dielectric properties of: a ε_r about 40, a Q×f about 17200 GHz, and a large positive τ_f value of 114.54 ppm/^{o}C when sintered at 1075^{o}C[12]. Considering that zirconium source is beneficial for the improvements of Q×f values in many systems. *i.e.* In trigonal solid solution $La_2(Zr_{1-x}Ti_x)_3(MoO_4)_9$ ($0 \leq x \leq 0.1$), improved dielectric properties of: ε_r = 10.33, Q×f = 80658 GHz, and τ_f = 3.48 ppm/^{o}C were obtained at x = 0.08[13]. Structure transformations between rutile and monoclinic phases take place in $Co_{0.5}(Ti_{1-x}Zr_x)_{0.5}NbO_4$ ceramics[14], and optimal microwave dielectric properties were achieved at x = 0.6: ε_r = 24.40, Q×f = 48599 GHz, and τ_f = 9.2 ppm/^{o}C. In monoclinic $MgZr(Nb_{1-x}Ta_x)_2O_8$ solid solutions, Q×f value was enhanced from 72842 to 88440 GHz when x = 0.1[5]. Therefore, Ti site of $Co_{0.5}Ti_{0.5}TaO_4$ ceramic is replaced by Zr^{4+} ion in this study. For instance, Wang reported synthesis of $CoZrTa_2O_8$ microwave dielectric ceramics, which is indexed with a pure monoclinic wolframite structure and shows a great temperature stability: ε_r ~ 23.54, Q×f ~ 20100 GHz, and τ_f ~ -8.72 ppm/^{o}C[15], However, our study on $Co_{0.5}Zr_{0.5}TaO_4$ ceramic using different cobalt source presents different phase compositions and dielectric performances.

2. Experimental

$Co_{0.5}Zr_{0.5}TaO_4$ microwave dielectric ceramics were prepared by traditional solid state technique. Raw materials of Co_2O_3 (99.0%), ZrO_2 (99.9%) and Ta_2O_5 (99.9%) oxides were quantified based on $Co_{0.5}Zr_{0.5}TaO_4$ chemical formula. Next, the mixtures were planetary ball-milled about 4 h in deionized water and then sieved from a 60-mesh screen mesh. After that, powders were calcined at 900~1100^{o}C. Calcined mixtures were then re-milled for 4 h and pressed into mold to form pellets with the assistance of polyvinyl alcohol (PVA) solution under a pressure of 20 MPa. Finally, pellets were sintered in the temperature range of 1100~1200 ^{o}C in air for 4 h.

For determining crystal structure and phase compositions, powder X-ray diffraction measurement was accomplished by using X-ray diffraction apparatus (X'pert Pro MPD, Phlips) equipped with Cu Kα radiation within the scanning angle of 2θ=10°~120°. Raman microscope with a model of LabRAM HR Evolution was used to analysis vibrational spectrum by using 514 nm line of a He-Ne laser source as an exciting wavelength. Micrograph of sintered samples was observed by a scanning electron microscopy (SEM, FEI Inspect F, the United Kingdom). Microwave dielectric performances were tested by Hakki-Coleman dielectric resonator method in the TE_{011} mode using a network analyzer (HP83752A, the United States). The τ_f value was calculated from the difference of resonant frequency between 25 ^{o}C and 85 ^{o}C.

3. Results and discussion

Raw materials of Co_2O_3, ZrO_2 and Ta_2O_5 were calcined at 900~1000^{o}C, and their powder X-ray diffraction (XRD) patterns after normalization were exhibited in Fig. 1. As one can clearly see, a trirutile $CoTa_2O_6$ phase (JCPDS # 32-0314) and a monoclinic ZrO_2 phase (JCPDS # 37-1484) coexist in temperature range of 900~1000^{o}C, illustrating that the chemical reaction takes place between Co_2O_3 and Ta_2O_5. Furthermore, characteristic diffraction peak intensities of (002) and (101) lattice planes of $CoTa_2O_6$ phase gradually increase, which means the content of $CoTa_2O_6$ phase increases.

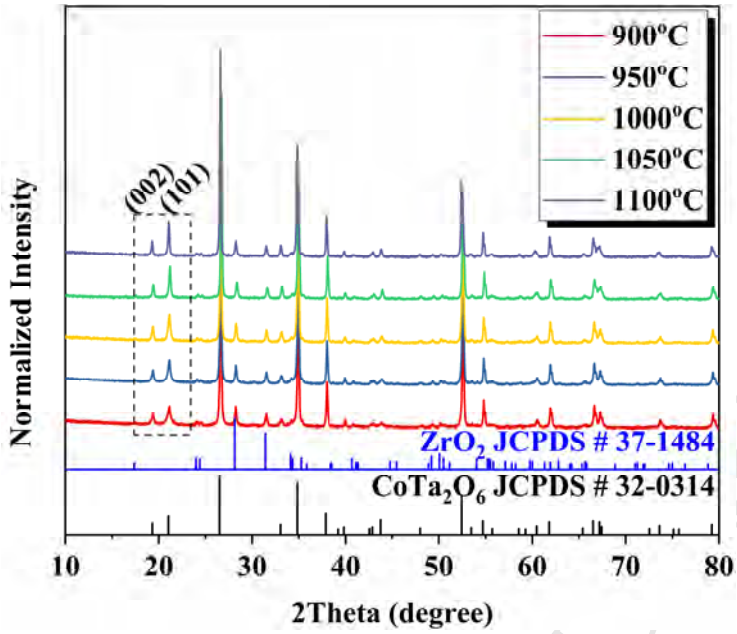

Fig.1 XRD patterns of $Co_{0.5}Zr_{0.5}TaO_4$ raw powders calcined at 900~1100°C

XRD patterns of $Co_{0.5}Zr_{0.5}TaO_4$ ceramic samples sintered at 1100~1200°C are exhibited in Fig. 2(a). Phase compositions are indexed as an coexistence of a monoclinic structure with P*2/c*(13) space group and a trirutile tetragonal structure with P*42/mnm*(136) space group. In addition, no diffraction peaks corresponding to other phases are detected. Rietveld refinement analysis equipped with GSAS-EXPGUI program were performed to quantify contents of crystalline phases and obtain important lattice parameters[16, 17]. Initial models of monoclinic and tetragonal structures were chosen from COD ID # 1520643[18] and COD ID # 1530640[19]. The XRD profile of ceramic sample sintered at 1200°C after refinement is shown in Fig. 2(b). Crystal parameters are listed in Table 1.

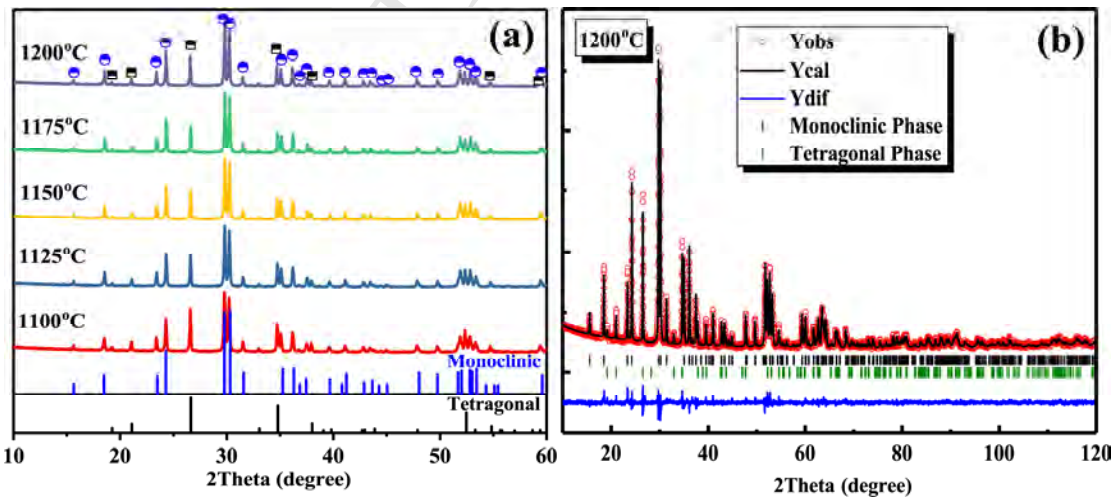

Fig.2 (a) XRD patterns of $Co_{0.5}Zr_{0.5}TaO_4$ ceramic samples sintered at 1100~1200°C; (b) XRD profile of $Co_{0.5}Zr_{0.5}TaO_4$ ceramic sample sintered at 1200°C after refinement, where the red circle and black line are observed and fitted intensities, vertical lines indicate the bragg positions of monoclinic and tetragonal phases, and blue line at the bottom is the difference between observed and fitted intensities

Table 1. Crystal parameters of monoclinic and tetragonal phases after refinement

Phase	ST	Lattice parameters						R_{wp}	R_p	χ^2
	(°C)	*a* (Å)	*b* (Å)	*c* (Å)	β (°)	V_{cell} (Å^3)	W_t (%)	(%)	(%)	
M-type	1100	4.8074	5.6891	5.1281	91.09	140.226	69.56	3.54	2.72	2.028
	1125	4.8026	5.6878	5.1240	91.12	139.940	74.82	3.61	2.75	2.072
	1150	4.7986	5.6892	5.1230	91.09	139.833	76.67	3.68	2.81	2.181
	1175	4.7988	5.6889	5.1219	91.11	139.800	76.53	3.79	2.84	2.368
	1200	4.8001	5.6938	5.1254	91.10	140.056	75.71	3.53	2.72	2.060
T-type	1100	4.7511	4.7511	9.2516	90.00	208.838	30.44			
	1125	4.7537	4.7537	9.2599	90.00	209.249	25.18			
	1150	4.7536	4.7536	9.2597	90.00	209.235	23.33			
	1175	4.7554	4.7554	9.2656	90.00	209.534	23.47			
	1200	4.7546	4.7546	9.2665	90.00	209.480	24.29			

M and T refers to monoclinic and tetragonal phases. ST is sintering temperature. W_t is weight fraction of each phase. R_{wp}, R_p and χ^2 are representative for reliability factor of weighted pattern, reliability factor of weighted pattern, and goodness of fit, respectively.

Micrographs of $Co_{0.5}Zr_{0.5}TaO_4$ samples sintered at 1125~1200°C are shown in Fig. 3. Corresponding grain size distributions are shown in Fig. 4. At 1125°C, in Fig. 3(a), the average size of grain is as small as 1.50 μm. With the sintering temperature increases from 1150°C to 1200°C, as shown in Fig. 3(b) to (d), growth of grain is promoted, and the grain size increased from 1.73~3.09 μm. It is worth mentioning that the difference between large and small grain are significant after 1175°C. Therefore, Energy Dispersive Spectrometer (EDS) analysis were performed on spot A and B, and the results are shown in Fig. 3(e) and (f). Based on the EDS analysis, molar ratio of Co: Ta is close to 1:2 in spot A, and no sign of zirconium element is detected. And molar ratio of Co: Zr: Ta is approximately 1:1:2 in spot B. Combined with XRD analysis above, the smaller grain belongs to trirutile tetragonal $CoTa_2O_6$ phase and the larger one may possible be the monoclinic phase with an atomic ratio close to $Co_{0.5}Zr_{0.5}TaO_4$.

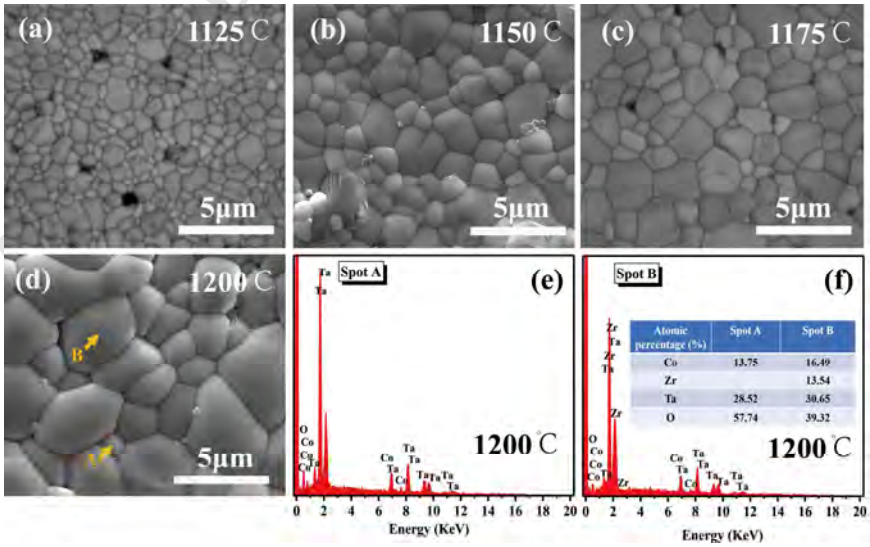

Fig.3 SEM images of $Co_{0.5}Zr_{0.5}TaO_4$ samples sintered at 1125~1200°C, the EDS results for spot A and B are exhibited in (e) and (f)

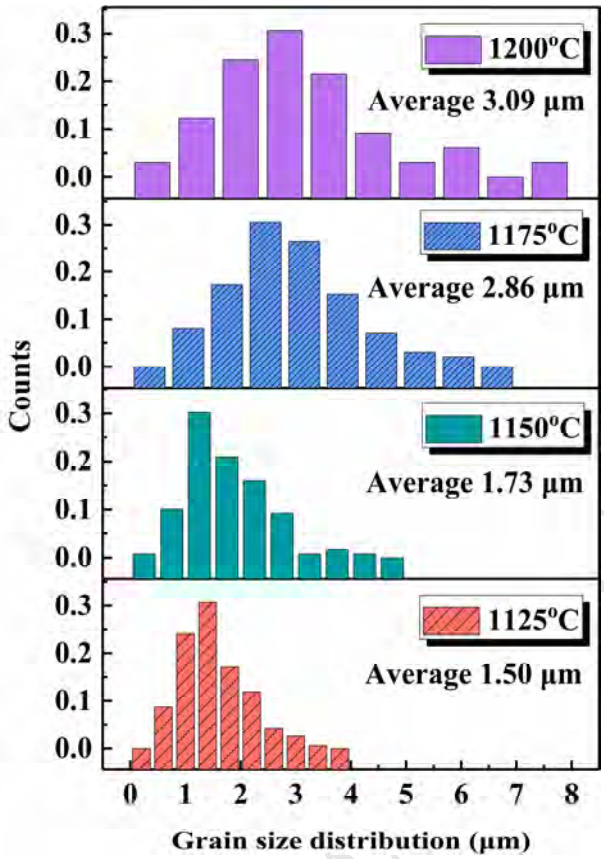

Fig.4 Grain size distributions of $Co_{0.5}Zr_{0.5}TaO_4$ samples sintered at 1125~1200°C

Raman spectroscopy is effective to analyze the crystal structure[20, 21]. Theoretically, based on group theory prediction, there are 18 and 16 Raman-active modes of another similar monoclinic phase $Mg_{0.5}Zr_{0.5}NbO_4$ ($10A_g + 8B_g$)[22] and tetragonal phase $CoTa_2O_6$ ($4A_{1g} + 2B_{1g} + 4B_{2g} + 6E_g$)[23], respectively. Experimental and fitted Raman spectrum of $Co_{0.5}Zr_{0.5}TaO_4$ sample when sintered at 1150°C is shown in Fig. 5. It is reasonable that experimental amounts of Raman-active bands are less than the total number of vibrational modes, for which some peaks with lower vibrational activities may become broaden or even covered by adjacent peaks with strong vibration intensities. Some observed Raman peaks after fitting are assigned according to monoclinic[22] and tetragonal $CoTa_2O_6$ phase[23], as listed in Table 2.

Table 2. Raman-active modes of $Co_{0.5}Zr_{0.5}TaO_4$ ceramic after fitting

M-phase	Mode (cm^{-1})	Assignment	T-phase	Mode (cm^{-1})
1	150.71	$B_{3g(4)}$	1	84.56
2	272.23	$B_{1g(3)}$	2	111.26
3	305.29	$B_{2g(1)}$	3	164.84
4	415.64	$B_{1g(1)}$	4	177.61
5	518.01		5	237.35
6	571.82	$B_{1g(2)}$	6	376.20
7	644.32	$A_{g(1)}$	7	384.18
8	745.10	$B_{3g(2)}$	8	472.41
9	858.64	$B_{3g(1)}$	9	674.19
10	868.21	$A_{g(2)}$		

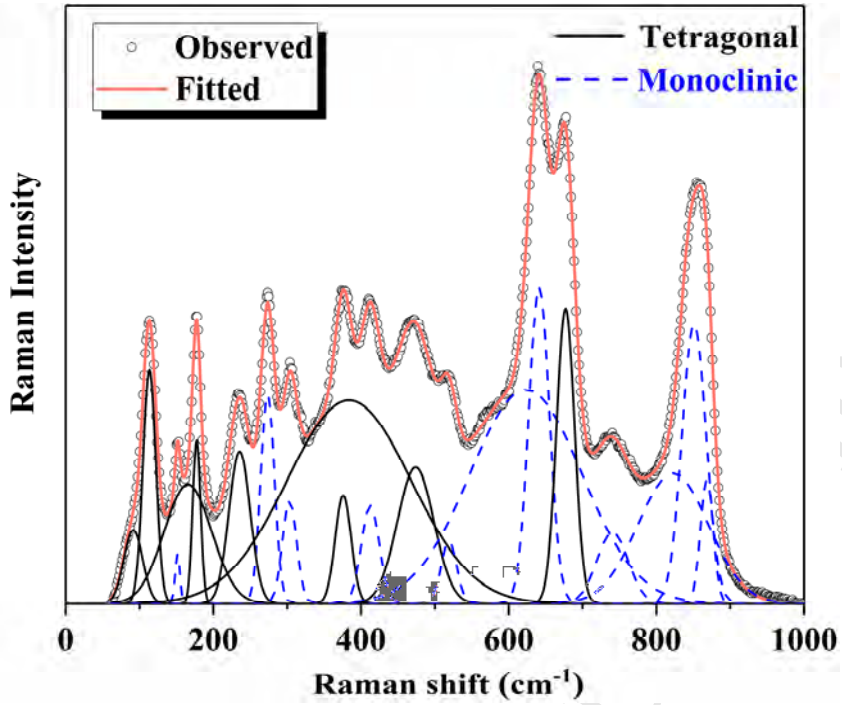

Fig.5 Experimental and fitted Raman spectrum of $Co_{0.5}Zr_{0.5}TaO_4$ ceramic sample sintered at 1150°C (Black solid line and blue dotted line are representatives for tetragonal and monoclinic phases, respectively)

It is reported that the intense Raman vibrational peaks dominate the Raman-active vibrational behaviors[24]. In our study, the most intense peaks locates in 644.32 cm^{-1}, 674.19 cm^{-1} and 858.64 cm^{-1}, while both the peaks at 644.32 cm^{-1} and 858.64 cm^{-1} belong to $A_{g(1)}$ and $B_{3g(1)}$ modes of monoclinic-type phase, which also demonstrates that monoclinic phase are coexisting as main crystalline phase. The Raman spectrum analysis provides evidence that monoclinic and tetragonal phases coexist in $Co_{0.5}Zr_{0.5}TaO_4$ ceramic sample, which supports the XRD analysis above.

Combined with the crystal structure analysis and EDS results above, schematic representations of monoclinic-type and trirutile tetragonal phases are presented in Fig. 6. Monoclinic $Co_{0.5}Zr_{0.5}TaO_4$ phase has a space group of P*2/c*(13) with Z=1 and a smaller cell volume V_{cell} about 139.833 $Å^3$. Co^{2+}/Zr^{4+} cations are randomly distributed at 2f Wyckoff site, while Ta^{5+} cation in 2e site. All cations are 6-coordinated, forming [Co/ZrO_6] and [TaO_6] octahedrons. Two types of O anion exist in octahedron: two shorter Ta-O2 bonds and four larger Ta-O1 bonds; two shorter Co/Zr-O1 bonds and four larger Co/Zr-O2 bonds. While in trirutile $CoTa_2O_6$ structure (Z=2) with P*42/mnm*(136) space group and a larger cell volume V_{cell} about 209.235 $Å^3$, it can be regarded as the extension of *c*-axis length of rutile phase. Similarly, Co^{2+} and Ta^{5+} cations are in 2a and 4e site, respectively. All cations form octahedrons as well, where bond lengths of Co-O2×4 bonds are larger than Co-O1×4; bond lengths of Ta-O1×2 bonds are larger than Ta-O2×4.

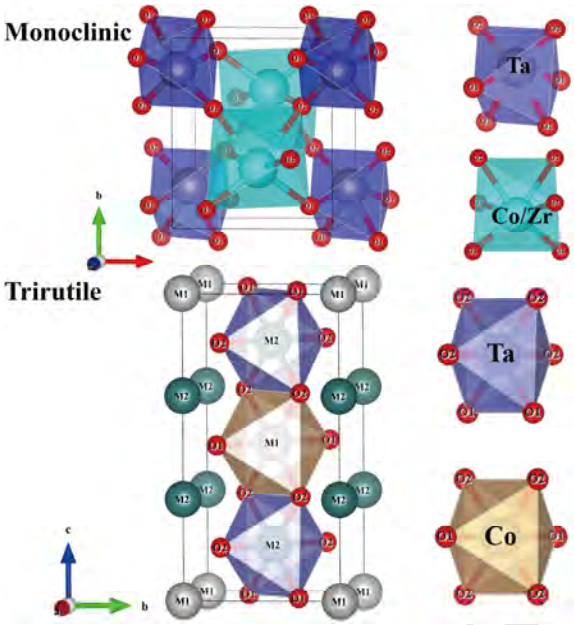

Fig.6 Schematic representations of monoclinic $Co_{0.5}Zr_{0.5}TaO_4$ and trirutile tetragonal $CoTa_2O_6$ phases

Since multiphase coexist in $Co_{0.5}Zr_{0.5}TaO_4$ ceramics, the importance of phase compositions and phase contents cannot be emphasized enough. It is widely accepted that the relative permittivity (ε_r) of composite ceramics is mainly influenced by the densification, phase composition and phase contents[20]. Therefore, the relative density and measured ε_r value are shown in Fig. 7(a). As can be seen, both the relative density and measured ε_r value show a consistent declining trend. Mentionable is that microstructure of $Co_{0.5}Zr_{0.5}TaO_4$ ceramic at 1125°C is not compact enough compared with that sintered at 1150°C, while relative density at 1125°C is larger. This phenomenon is attributed to the phase contents of tetragonal phase. Calculated theoretical density of tetragonal $CoTa_2O_6$ phase is about 8.203 g/cm^3, which is larger than 7.595 g/cm^3 of monoclinic phase, and contents of tetragonal phase at 1125°C is larger than 1150°C. Thus, the relative density still decreases.

Furthermore, phase compositions and phase contents should also be taken into consideration for ε_r value by following the mixture rules[25]:

$$\ln \varepsilon_{cal} = V_M \ln \varepsilon_M + V_T \ln \varepsilon_T \quad (1)$$

$$Q \times f = V_M \left(Q \times f\right)_M + V_T \left(Q \times f\right)_T \quad (2)$$

$$\tau_f = V_M \tau_{fM} + V_T \tau_{fT} \quad (3)$$

where V represents the volume fraction of each crystalline phase. M and T refers to monoclinic and tetragonal phases, respectively. According to reported literatures, microwave dielectric properties for M-type $MgZrNb_2O_8$ phase: ε_r = 26, Q×f = 120816 GHz, τ_f = -50.2 ppm/°C and T-type phase: ε_r = 29, Q×f = 2900 GHz, τ_f = 23 ppm/°C are selected here[22, 26].

In addition, measured ε_r should take the influence of porosity (P) into consideration *via* Bosman and Havinga correction[27]:

$$\varepsilon = \varepsilon_r \left(1+1.5P\right) \quad (4)$$

$$P = 1-\rho_{relative} \quad (5)$$

Comparisons between microwave dielectric properties are shown in Fig. 7(b) to (d). In Fig. 7(b), variation of calculated ε_r value by using reported value is also similar with measured ε_r after considering the porosity. Both Fig. 7(a) and (b) imply that variation of densification, phase composition and phase contents are non-negligible for the developments of ε_r value.

The variation of Q×f value in composites is susceptible to densification, phase compositions and average grain size[28, 29]. In Fig. 7(c), considering the existing multiphase, calculated Q×f value varies consistently with measured value. However, theoretical Q×f value slightly declines after 1150°C, while measured one drops dramatically. This phenomenon is ascribed to the decrease of densification and abnormal growth of grain.

The τ_f value, which reflects temperature stability of microwave dielectric ceramics, is determined by the following correlation[27]:

$$\tau_f = -\left(\tau_\varepsilon/2\right)-\alpha_L \quad (6)$$

where τ_ε and α_L are temperature coefficient of dielectric constant and thermal expansion coefficient. In dielectric ceramics, α_L is normally regarded as a constant value. Therefore, τ_ε provides great contributions to τ_f value[30]. Specifically, dielectric polarizability is responsible for variations of τ_f value. Previous studies in $Zn_{0.15+0.35x}Ti_{0.55-0.05x}Nb_{0.3+0.7x}O_{2+2x}$ and $Zn_{0.15}Nb_{0.3}(Ti_{1-x}Zr_x)_{0.55}O_2$ ceramics demonstrate that the τ_f value is consistent with variation of ε_r value[31, 32]. Generally speaking, the densification, phase compositions, phase contents are also crucial for developments of τ_f value. As one could expect from Fig. 7(a), (b) and (d), variation of measured τ_f value is similar with relative density, ε_r value and calculated τ_f value.

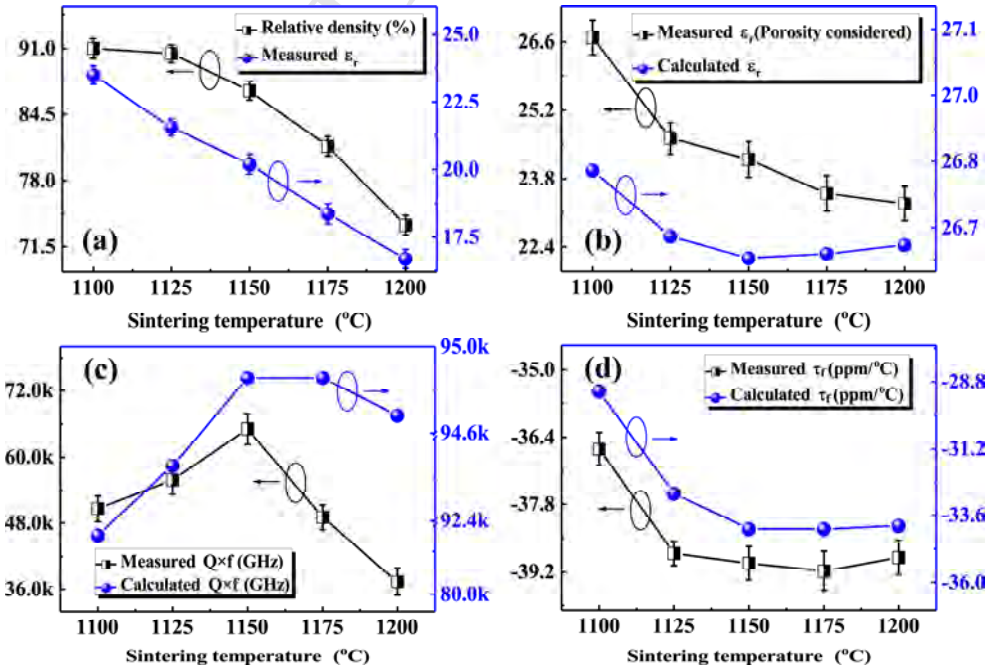

Fig.7 Microwave dielectric properties of $Co_{0.5}Zr_{0.5}TaO_4$ ceramics

4. Conclusion

In this work, a novel $Co_{0.5}Zr_{0.5}TaO_4$ ceramic was reported. The crystal structure, phase composition, Raman spectrum and microwave dielectric properties were investigated. Based on the powder X-ray diffraction measurement, Rietveld refinement analysis and Raman spectrum analysis, a coexistence of monoclinic structure and trirutile tetragonal phase is confirmed in $Co_{0.5}Zr_{0.5}TaO_4$ ceramics. Developments of microwave dielectric properties of $Co_{0.5}Zr_{0.5}TaO_4$ samples in the temperature range of 1100~1200^{o}C are mainly affected by densification, growth of grain, phase compositions and phase contents. Combination great microwave dielectric properties of $Co_{0.5}Zr_{0.5}TaO_4$ ceramics were achieved when sintered at 1150^{o}C: ε_r = 20.19, Q×f = 65125 GHz, τ_f = -39.02 ppm/^{o}C.

Acknowledgement

This work was supported by the National Natural Science Foundation of China (Grant number 51872037).

References

[1] Y.H. Zhang, J.J. Sun, N. Dai, Z.C. Wu, H.T. Wu, C.H. Yang, Crystal structure, infrared spectra and microwave dielectric properties of novel extra low-temperature fired $Eu_2Zr_3(MoO_4)_9$ ceramics, J. Eur. Ceram. Soc, 39 (2019) 1127-1131.

[2] B. Zhang, L. Li, W. Luo, Chemical substitution in spinel structured $LiZnNbO_4$ and its effects on the crystal structure and microwave performance, J. Alloys Compd, 771 (2019) 15-24.

[3] J. Bi, Y. Niu, H. Wu, $Li_4Mg_3Ti_2O_9$: A novel low-loss microwave dielectric ceramic for LTCC applications, Ceram. Int, 43 (2017) 7522-7530.

[4] B. Zhang, L. Li, W. Luo, Oxygen vacancy regulation and its high frequency response mechanism in microwave ceramics, J. Mater. Chem. C, 6 (2018) 11023-11034.

[5] M. Xiao, J. Lou, Z. Zhou, Q. Gu, Y. Wei, P. Zhang, Crystal structure and microwave dielectric properties of Ta^{5+} substituted $MgZrNb_2O_8$ ceramics, Ceram. Int, 43 (2017) 15567-15572.

[6] H. Wu, E.S. Kim, Characterization of crystal structure and microwave dielectric properties of $AZrNb_2O_8$ (A=Zn, Co, Mg, Mn) ceramics based on complex bond theory, Ceram. Int, 42 (2016) 5785-5791.

[7] D.W. Kim, K.H. Ko, D.K. Kwon, K.S. Hong, Origin of microwave dielectric loss in $ZnNb_2O_6$-TiO_2, J. Am. Ceram. Soc, 85 (2002) 1169-1172.

[8] H.T. Wu, Z.B. Feng, Q.J. Mei, J.D. Guo, F.F. Hou, P.S. Li, X.S. Jiang, Synthesis, characterization, and microwave dielectric properties of $ZnTiTa_2O_8$ ceramics with ixiolite structure obtained through the aqueous sol-gel process, Ceram. Int, 41 (2015) 7645-7650.

[9] X. Lyu, L. Li, S. Zhang, H. Sun, S. Li, J. Ye, B. Zhang, et al., A new low-loss dielectric material $ZnZrTa_2O_8$ for microwave devices, J. Eur. Cera. Soc, 36 (2016) 931-935.

[10] W.S. Xia, Z.W. Zuo, L.Y. Zhang, L.W. Shi, Y. Wang, S.E. Jin, Y.P. Xu, Extrinsic effects on microwave dielectric properties of high-Q $MgZrTa_2O_8$ ceramics, J. Mater. Sci. Mater. Electron, (2016) 27(11): 11325-11330.

[11] Y. Wang, L.Y. Zhang, S.B. Zhang, W.S. Xia, L.W. Shi, Sintering behavior and microwave dielectric properties of $MgZrTa_2O_8$ ceramics with fluoride addition, Mater. Lett. 219 (2018) 233-235.

[12] H. Yang, S. Zhang, Y. Chen, H. Yang, Y. Yuan, E. Li, Crystal chemistry, Raman spectra, and bond characteristics of trirutile-type $Co_{0.5}Ti_{0.5}TaO_4$ microwave dielectric ceramics, Inorg. Chem. 58 (2018) 968-976.

[13] Y. Zhang, H. Wu, Crystal structure and microwave dielectric properties of $La_2(Zr_{1-x}Ti_x)_3(MoO_4)_9$ ($0 \leq x \leq 0.1$) ceramics, J. Am. Ceram. Soc, 102 (2019) 4092-4102.

[14] Y. Li, X. Lu, Y. Zhang, Y. Zou, L. Wang, H. Zhu, Z. Fu, et al., Characterization of $Co_{0.5}(Ti_{1-x}Zr_x)_{0.5}NbO_4$ microwave dielectric ceramics based on structural refinement, Ceram. Int, 43 (2017) 11516-11522.

[15] Y. Wang, S.B. Zhang, T.L. Tang, W.S. Xia, L.W. Shi, Investigation on microwave dielectric properties of new low-loss $CoZrTa_2O_8$ ceramics, Mater. Lett, 231 (2018) 1-4.

[16] B. Toby, EXPGUI, a graphical user interface for GSAS, J. Appl. Crystallogr, 34 (2001) 210-213.

[17] A.C. Larson, R.B. Von Dreele, General Structure Analysis System (GSAS), Los Alamos National Laboratory Report LAUR 86-748. (2004)

[18] M.A. Dahlborg, G. Svensson, Structural changes in the system $Zn_{1-x}Cd_xWO_4$, determined from single crystal data, Acta. Chem. Scand, 53 (1999) 1103-1109.

[19] J.N. Reimers, J.E. Greedan, C.V. Stager, R. Kremer, Crystal structure and magnetism in $CoSb_2O_6$ and $CoTa_2O_6$, J. Solid. State. Chem, 83 (1989) 20-30.

[20] Z. Fang, B. Tang, Y. Yuan, X. Zhang, S. Zhang, Structure and microwave dielectric properties of the $Li_{2/3(1-x)}Sn_{1/3(1-x)}Mg_xO$ systems (x = 0-4/7), J. Am. Ceram. Soc, 101 (2018) 252-264.

[21] D. Zhou, L.X. Pang, J. Guo, Z.M. Qi, T. Shao, Q.P. Wang, H.D. Xie, et al., Influence of Ce substitution for Bi in $BiVO_4$ and the impact on the phase evolution and microwave dielectric properties, Inorg. Chem, 53 (2014) 1048-1055.

[22] J. Zhang, R. Zuo, Y. Cheng, Relationship of the structural phase transition and microwave dielectric properties in $MgZrNb_2O_8$–TiO_2 ceramics, Ceram. Int, 42 (2016) 7681-7689.

[23] H. Haeuseler, Infrared and Raman spectra and normal coordinate calculations on trirutile-type compounds, Spectrochim. Acta. A, 37 (1981) 487-495.

[24] D. Zhou, L.X. Pang, J. Guo, H. Wang, X. Yao, C. Randall, Phase evolution, Phase transition, Raman spectra, Infrared spectra, and microwave dielectric properties of low temperature firing $(K_{0.5x}Bi_{1-0.5x})(Mo_xV_{1-x})O_4$ ceramics with scheelite related structure, Inorg. Chem, 50 (2011) 12733-12738.

[25] K. Fukuda, R. Kitoh, I. Awai, Microwave characteristics of TiO_2-Bi_2O_3 dielectric resonator, Jpn. J. Appl. Phys, 32 (1993) 4584-4588.

[26] H.J. Lee, I.T. Kim, K.S. Hong, Dielectric properties of AB_2O_6 compounds at microwave frequencies (A=Ca, Mg, Mn, Co, Ni, Zn, and B=Nb, Ta), Jpn. J. Appl. Phys, 36 (1997) 1318-1320.

[27] A.J. Bosman, E.E. Havinga, Temperature dependence of dielectric constants of

cubic ionic compounds, Phys. Rev, 129 (1963) 1593-1600.

[28] L.X. Pang, D. Zhou, Modification of $NdNbO_4$ microwave dielectric ceramic by Bi substitutions, J. Am. Ceram. Soc, 102 (2019) 2278-2282.

[29] C.F. Tseng, Microwave dielectric properties of low loss microwave dielectric ceramics: $A_{0.5}Ti_{0.5}NbO_4$ (A=Zn, Co), J. Eur. Ceram. Soc,34 (2014) 3641-3648.

[30] P.P. Ma, X.Q. Liu, F.Q. Zhang, J.J. Xing, X.M. Chen, $Sr(Ga_{0.5}Nb_{0.5})_{1-x}Ti_xO_3$ Low−loss microwave dielectric ceramics with medium dielectric constant, J. Am. Ceram. Soc, 98 (2015) 2534-2540.

[31] H. Yang, S. Zhang, H. Yang, X. Zhang, E. Li, Structural evolution and microwave dielectric properties of $xZn_{0.5}Ti_{0.5}NbO_4$-$(1–x)Zn_{0.15}Nb_{0.3}Ti_{0.55}O_2$ ceramics, Inorg. Chem, 57 (2018) 8264-8275.

[32] H. Yang, S. Zhang, H. Yang, Y. Chen, Y. Yuan, E. Li, Effects of ZrO_2 substitution on crystal structure and microwave dielectric properties of $Zn_{0.15}Nb_{0.3}(Ti_{1-x}Zr_x)_{0.55}O_2$ ceramics, Ceram. Int, 44 (2018) 22710-22717.